Biosensors and Bioelectronics 129 (2019) 79–86

Contents lists available at ScienceDirect

Biosensors and Bioelectronics

journal homepage: www.elsevier.com/locate/bios

Plasmonic biosensors for bacterial endotoxin detection on biomimetic C-18 supported fiber optic probes

Hariharan Manoharan[a], Prasanta Kalita[b], Shalini Gupta[b], V.V.R. Sai[a,*]

[a] Department of Applied Mechanics, Indian Institute of Technology Madras, Chennai 600036, India
[b] Department of Chemical Engineering, Indian Institute of Technology Delhi, New Delhi 110016, India

ARTICLE INFO

Keywords:
Endotoxin
Lipopolysaccharide
Polymyxin B
Gold nanoparticles
Plasmonic sandwich assay
U-bent fiber optic sensor

ABSTRACT

Bacterial endotoxins such as lipopolysaccharides (LPS) are major contaminants of most pharmaceutical and consumer products. We report an antibiotic-mediated plasmonic biosensor for LPS detection based on a facile U-bent fiber optic probe (UFOP) technology. Biomimetic self-assembled layer of octadecyltrichlorosilanes (OTS) were functionalized on the surface of optical fiber probes to hydrophobically entrap LPS from aqueous solutions. The binding of LPS molecules was monitored in real-time by measuring the change in refractive index (RI) in the evanescent layer. To add specificity and signal amplification, the bound LPS molecules were further tagged with antimicrobial polymyxin-B conjugated gold nanoparticles (PMB-AuNPs) in a sandwich format. The assay was extensively optimized by investigating the role of experimental parameters like OTS concentration, incubation time and addition of a silver reduction step at the end of the assay. The lower limit of detection (LOD) for LPS was found to be 0.4 ng/mL with a 36-fold improved sensitivity upon silver enhancement. The total assay time was 1 h. The assay was also found to be highly specific in the presence of common biopharmaceutical components and could thus serve as an efficient endotoxin detection platform for quality control testing during therapeutic development.

1. Introduction

Bacteria continue to be the preferred choice for host expression in the biopharmaceutical industry to produce a wide range of recombinant proteins, therapeutic drugs, amino acids, biofuels and biopolymers (Chen et al., 2013). In fact, almost 30% of all the commercially available biologics including vaccines, peptides and hormones are derived from genetically engineered *E. coli* (Ferrer-miralles et al., 2009; Huang et al., 2012). However, endotoxin contamination in these products still remains a serious issue (Mamat et al., 2015). During the manufacturing process, LPS can be liberated into the products at any stage of microbial growth, division, death and lysis (Kalyanpur, 2002). LPS is a class of large complex molecules (10–20 kDa) uniquely found in the outer membrane of the Gram-negative bacteria such as *E. coli, Salmonella* and *Pseudomonas*. It is indispensable for bacterial survival as it provides membrane integrity, permeability and self-defense. The outer membrane envelope of *E. coli* typically consists of a million copies of LPS covering almost three-fourths of its cell surface (Whitfield and Trent, 2014). Structurally, this amphiphilic molecule is a glycolipid made up of a highly conserved lipid A moiety, an oligopolysaccharide rich core and repeating O-antigen units. The lipid A moiety is responsible for pathogenesis and virulence of LPS whereas, the O-antigens provide protection to the Gram-negative bacteria against host defense (Bryant et al., 2010). This chemical composition of LPS gives it a remarkably high stability to withstand high temperatures and pressures (Gorbet and Sefton, 2005). Entry of LPS into the human circulation even at sub-nanomolar levels can cause endotoxemia, septic shock and multiorgan failure (Angus and Poll, 2013).

The current standard tests for LPS detection are the Limulus Amebocyte Lysate (LAL) assays. These tests are quite sensitive but limited in application due to interfering molecules such as Ethylene Diamine Tetra Acetic acid (EDTA), glucans, proteases, phenols and also pH conditions (Dawson, 1998; FDA, 2012). Further, Enzyme-Linked Immunosorbent Assays (ELISAs) for LPS detection are seldomly reported owing to the difficulties in developing specific primary and secondary antibodies against LPS (Grallert et al., 2011). Several alternative attempts have been reported to detect LPS using electrochemical, optical and piezoelectric sensors (Das et al., 2014). The important aspect in all of these techniques is to identify specific receptors that efficiently capture LPS by exploiting its unique structural architecture. Many studies have targeted the negatively charged glyco-core (phosphorylated) of LPS for binding to positively charged receptors including

* Corresponding author.
E-mail address: vvrsai@iitm.ac.in (V.V.R. Sai).

https://doi.org/10.1016/j.bios.2018.12.045
Received 19 October 2018; Received in revised form 18 December 2018; Accepted 21 December 2018
Available online 03 January 2019
0956-5663/

polylysine and histidine (Petsch and Anspach, 2000). On the other hand, the hydrophobic lipid A is utilized to anchor LPS on a surface modified with polyethylene, polyvinylidene fluoride and polytetrafluoroethylene (Williams et al., 2007). Moreover, LPS molecules are also known to form stable micelles and other lamellar, cubic hexagon *etc.* supramolecular structures depending on the surrounding environmental conditions by means of self-aggregation through their hydrophobic chain groups (Seydel et al., 1993). In an interesting study, Schneck et al., have exploited this property of LPS to anchor them to a hydrophobically functionalized planar silica substrate to study the influence of divalent cations on LPS conformation (Schneck et al., 2009). Silin et al. and A.L. Plant have demonstrated the use of alkanethiol (C18) monolayers to study the hybrid lipid bilayer formation using the surface plasmon resonance technique. The LPS tethering to alkyl monolayered surface is similar to the lipid bilayer formation found in bacterial membranes (Plant, 1999; Silin et al., 2002). Each molecule of LPS derived from *E. coli* O55:B5 contains six acyl chains of varying carbon length between C12 to C14 (Bergstrand et al., 2006). These chains can interact with and anchor to the C18 alkyl chains present on the surface forming a bilayer, driven by strong thermodynamic interactions (Kalita et al., 2017). These reports indicate that hydrophobic coatings, such as long alkyl chain molecules can serve as useful receptors to sequester LPS on a solid support. On the other hand for LPS labeling (receptor), we have utilized polymyxin-B (PMB), a cationic cyclic peptide antibiotic that selectively neutralizes negatively charged LPS at pH 7.4 through electrostatic and hydrophobic interactions (Velkov et al., 2010). Compared to expensive antibody-based LPS detection, C18 alkyl chain mediated capturing technique combined with PMB antibiotic labeling can be a viable and cost–effective alternative.

Over the last decade or so, UFOP-based chemical and biological sensors have become widely popular for detecting analytes such as biomarkers (Ramakrishna and Sai, 2016), metabolites (Srivastava et al., 2012), proteins (Khatri et al., 2018), DNA (Gowri and Sai, 2017), whole cells (Arcas et al., 2018) as well as physical parameters such as RI (Divagar et al., 2018) and pH (Chandra and Mukherji, 2018) changes. The UFOP sensing platforms offer a wide range of benefits such as high sensitivity, ease of handling, miniaturization, portability, affordability and most importantly, real-time, label-free monitoring of biomolecular binding events. In these systems, the light is guided by the phenomenon of total internal reflection (TIR), wherein the light undergoes multiple reflections at the core-clad interface of the optical fiber with a minimum loss. As a result of this TIR, there exists an exponentially decaying electromagnetic field called the evanescence waves at the interface. At the decladded U-region of the fiber, this evanescence wave is utilized to sense the properties of its surrounding medium. Penetration depth of this evanescence field is much higher in UFOPs compared to a straight fiber which results in enhanced sensitivities (Gupta and Kant, 2018).

We have earlier reported the use of OTS (C18) to hydrophobically entrap LPS on glass slides and detect it in a dot blot bioassay format (Kalita et al., 2015). In the current work, we have extended this concept to the fabrication of a real-time, plasmonic biosensor that can operate both in a label-free (direct) and sandwich format. The plasmonic sandwich assay comprises of three steps (Fig. 1A). First, the LPS is trapped hydrophobically on an OTS-functionalized UFOP that enables us to record LPS binding in real time (direct mode). Second, the bound LPS is tagged with highly specific PMB-AuNP labels and their plasmonic absorbance response is measured under evanescence wave excitation (sandwich assay). Here, the absorbance signal is directly proportional to the LPS concentration. Third, a simple silver reduction step is added at the end of the assay to amplify its sensitivity manifold. In the following sections, we demonstrate the detailed design, development and optimization of the assay and establish its potential as a simple and portable sensor for LPS detection in aqueous samples.

2. Materials and methods

2.1. Materials

Lyophilized LPS (*Escherichia coli* O55:B5), OTS, toluene, hydrogen peroxide, sulphuric acid, gold (III) chloride ($HAuCl_4$), sodium citrate dihydrate, human IgG and silver enhancer kit (Sigma Aldrich, India); Fluorescent LPS (LPS-Alexa 488, L23351) (Thermofisher Scientific, India); PMB (TCI Chemicals, Japan); Extra pure grade L-threonine, L-tyrosine and lactic acid (SRL chemicals, India.); Non-pyrogenic normal saline (NS) (0.9% w/v or 150 mM NaCl) (Fresenius Kabi, India); Dextrose NS (DNS) water for injection (5% w/v dextrose with 0.9% w/v NaCl) (Otsuka Pharmaceuticals, India); Step-index multimode silica optical fibers of 0.39 NA (numerical aperture) and 200 μm core diameter (FT200UMT), PM-100-USB power meter interfaced with a compact fiber photodiode (S150C), green light emitting diode (LED, 525 nm), bare fiber terminator (BFT1) with a multimode SMA905 connector (Thorlabs Inc., USA). All experiments were performed in endotoxin free (EF) water (< 0.001 EU/mL) (Hyglos GmbH, Germany) at room temperature (~25 °C). The chemicals were used as received.

2.2. UFOP fabrication

Straight silica optical fibers of length 30 cm were decladded in the middle over a length of 1 cm by mechanically stripping off both the fiber buffer coating and the polymer cladding using a sharp razor. The uncovered portion was thoroughly wiped with an acetone-wet tissue followed by ethanol cleansing to expose the silica core. The decladded silica fiber was then bent into a U-shape of 1.0 ± 0.2 mm diameter by exposing it to a butane torch (Fig. S1, Supplementary material). This bend diameter was chosen based on our previous studies (*unpublished*) that showed maximum RI sensitivity in the visible wavelength at this diameter for a 200 μm silica core fiber. The fiber ends were also polished for better light coupling.

2.3. Immobilization of OTS receptors

The UFOPs were cleaned by dipping in an acidic piranha solution (70% H_2SO_4 + 30% H_2O_2) for 1 h followed by extensive washing with DI water and drying in a hot air oven at 100 °C for 1 h. To ensure uniform silane coating, the fibers were immediately dipped in a freshly prepared solution of 10 mM OTS in toluene at 28 °C under nitrogen atmosphere. After 12 h, the OTS-functionalized probes were sonicated for 5 min and washed with excess toluene to remove any unbound OTS molecules. In order to remove water molecules, the probes were dried at 100 °C for 30 min and stored under nitrogen atmosphere until further use. For preliminary surface characterization studies, 5 cm long straight silica optical fibers with a 2 cm long decladded portion were prepared separately.

2.4. Preparation of LPS solutions

A stock solution LPS (1 mg/mL) was prepared by reconstituting LPS powder in EF water. The LPS solutions were vortexed and sonicated at 37 °C for 20 min (a crucial step to disrupt micelle formation) and then aliquoted into lower concentrations by serial dilution. Glass vials were used throughout our experiments and plasticware was avoided as much as possible because LPS is known to stick to polymeric surfaces (Ryan, 2008).

2.5. Preparation of PMB-AuNP labels

AuNPs were synthesized by the well-known Frens method (Frens, 1973). Briefly, 100 mL of aqueous 0.25 mM $HAuCl_4$ solution was boiled and to this, 10 mL of freshly prepared 1% (w/v) aqueous sodium citrate solution was added. The color of the solution immediately turned dark

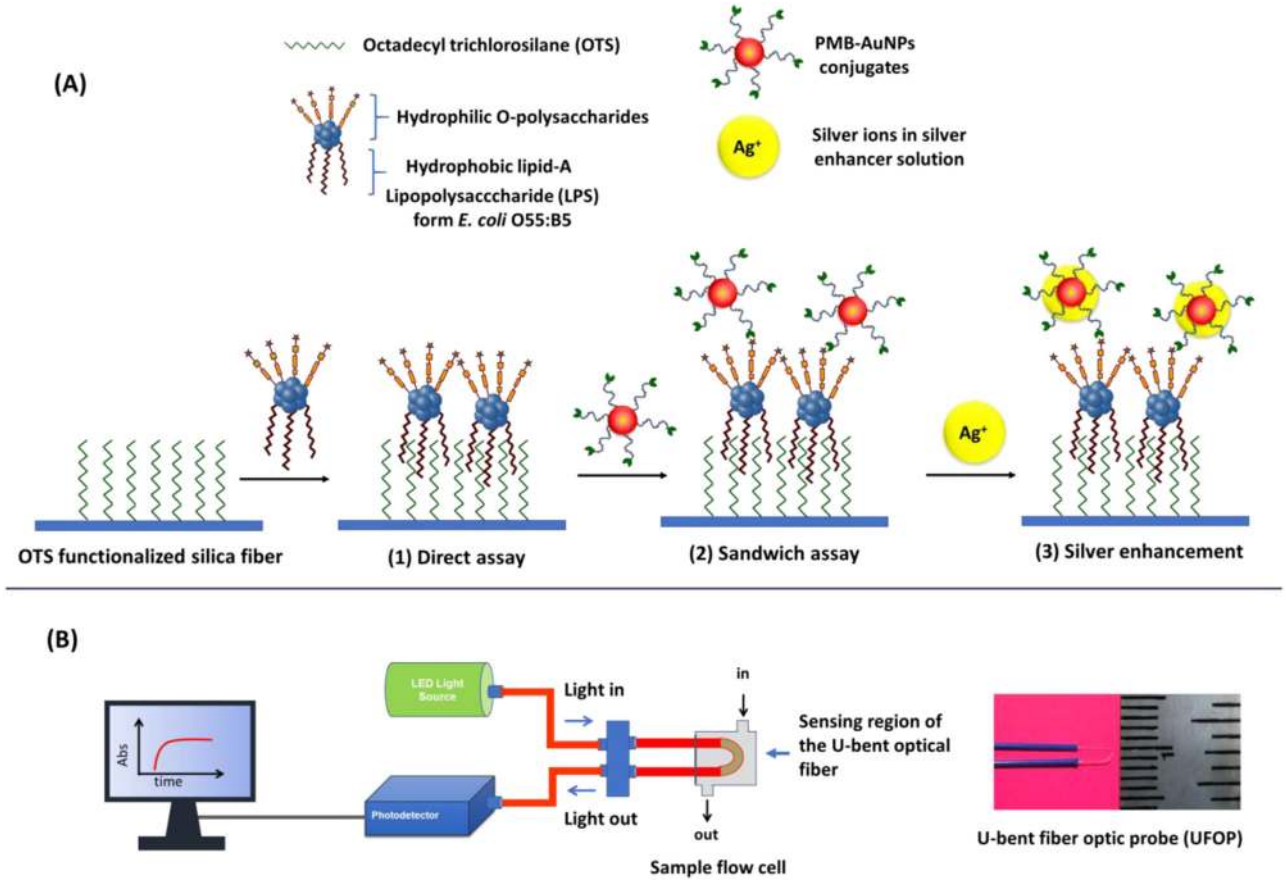

Fig. 1. Schematic of (A) LPS bioassay on a silica UFOP surface functionalized with OTS molecules and (B) optical setup used for LPS detection with an actual photograph of a UFOP with a bend diameter of 1 mm.

purple and then to ruby red on further boiling, indicating the successful formation of AuNPs. To 5 mL of this AuNP suspension (optical density, O.D. = 1.0), 50 µL of 5 µM PMB was added and incubated for 1 h. The excess PMB was removed by centrifuging the particles thrice at 9050 RCF (relative centrifugal force) for 30 min each. The final PMB-AuNP pellet was resuspended in EF water to an O.D. of 1.0 and stored at 4 °C until further use.

2.6. Optical setup and bioassay performance

One end of the UFOP was coupled to a green LED light source driven by a constant current source and the other end was coupled to a compact fiber photodiode. Both ends were mounted using bare fiber adaptors and SMA connectors. The U-bent sensing probe region was placed inside a custom-made glass capillary flow cell (under static conditions) with a sample holding capacity of 200 µL (Fig. 1B). The photodiode was interfaced to a computer through a USB power meter console and the temporal absorbance response at 525 nm wavelength was recorded using the PM100 utility software (version 4.9). The OTS functionalized UFOPs were incubated (~25 min) in different concentrations of LPS solution and LPS binding was monitored in real-time in a label-free manner. All samples were sonicated for 5 min at 35 °C prior to the experiments and a fresh OTS-treated UFOP was used for each LPS concentration. Next, the UFOPs were dipped in a PMB-AuNP suspension for 30 min. Finally, the probes were immersed (~3 min) in 50 µL of silver enhancer solution (1:1 v/v initiator: silver). At the end of each step, UFOPs were washed twice with excess EF water to remove unbound molecules. Each experiment was repeated at least thrice and the mean and standard deviations were obtained. The LOD of the assay was calculated using the formula LOD = 3Q/S, where Q is the standard deviation value for the blank and S is the sensitivity for the concentration range of 0.1–100 ng/mL LPS. Additionally, in case of fluorescent LPS experiments, the OTS functionalized straight probes were incubated with 1 µg/mL fluoro-LPS solution for 2 h followed by gentle washing with EF water.

2.7. Particle and surface characterization

2.7.1. Transmission electron microscopy (TEM)

The size and morphology of the AuNPs were determined using TEM (FEI Tecnai T20) at 200 kV. The samples were prepared by drop-casting 5 µL of a dilute AuNP suspension on carbon-coated copper grids with 200 mesh size (Make electron microscopy science, USA). The mean particle diameter was found to be 17 ± 3 nm from the particle size distribution of ~130 particles using the open-source software ImageJ (Fig. S6, Supplementary material).

2.7.2. UV–visible spectroscopy

The UV–visible absorption spectra were recorded at a scan rate of 600 nm/min using Agilent Cary 60 spectrophotometer (190–1100 nm). The concentration of the AuNP suspension (O.D. = 1.0) was estimated using the Beer-Lambert's law. The path length used was 1 cm and the extinction coefficient of (7.8×10^8 M^{-1} cm^{-1}) at maximum absorbance (523 nm) was obtained from the literature (Jana et al., 2001).

2.7.3. Raman spectroscopy

The Raman scattering spectra of OTS-coated silica fibers were collected using LabRam HR800 (Horiba Jobin Yvon, France) using a long working distance 50 × lens objective and a diode pumped solid state (DPSS) laser source operated at 532 nm. The laser power was kept at

20 mW and the accumulation time was varied between 10 and 20 s. The vibrational modes of -CH_2 stretching were measured between 2700 and 3000 cm^{-1}. A total of nine different spots were analyzed from three different silica fibers.

2.7.4. Fluorescence microscopy

Clean decladded 2 cm long straight silica fibers functionalized with varying OTS concentrations were incubated with 1 μg/mL of LPS-Alexa 488 for 2 h followed by gentle washing with EF water. The fibers were then imaged under 10 × magnification using an Olympus BX53 fluorescence microscope fitted with a Hamamatsu flash 4.0 CMOS camera (2 s exposure, 49.8 gain) with the excitation and emission wavelengths at 495 and 530 nm, respectively. A total of 10 fluorescence images were recorded from four different probes for each OTS concentration. The fluorescence signals were quantified using ImageJ software by selecting an area of 200 × 200 μm^2 on the fiber surface.

2.7.5. Dynamic contact angle (DCA) measurements

Water contact angles of bare, OTS, OTS/LPS immobilized probe surfaces (straight fiber) were measured using the Wilhelmy plate technique (Sigma700/701 Attension Force Tensiometer). A straight fiber was first mounted on the sample holder and then immersed into or emmersed from the wetting liquid at a constant rate of 4 mm/min (Fig. S2, Supplementary material). The corresponding advancing (θ_A) and receding (θ_R) contact angles were then estimated using a standard formula (see Supplement information). Measurements were made for three fiber probes.

2.7.6. Scanning electron microscopy (SEM) and elemental analysis

The probes were gold sputtered for 10 s to obtain a continuously conducting surface. Then the probes were mounted on the chuck and a carbon tape was laid to provide a conducting path in order to minimize the charging of the probes. The surface morphology of the U-bent fiber probes was imaged using SEM (Hitachi S4800) at different voltages (kV). The energy dispersive X-ray (EDAX) technique was used to analyze the elemental composition of the fiber probe surface. A total of three probes were analyzed and the data were reported as an average of measurements taken at three different positions on each probe.

3. Results and discussion

3.1. Label-free direct assay for LPS detection

3.1.1. Probe functionalization with OTS

The first set of experiments was performed by varying the OTS coverage on the sensor surface. The OTS packing density can have a profound effect on the conformation order of the alkyl chains which can in turn play a crucial role in the retention of LPS on the surface (Liao and Pemberton, 2008). Self-assembled OTS layers were formed on the hydroxylated silica surface of the straight decladded fibers by treating them with increasing concentrations of OTS (Kulkarni et al., 2005; Mcgovern et al., 1994). To assess the conformational ordering of C18 alkyl groups on the fiber probes, we compared the Raman scattering intensity of CH_2-antisymmetric ($\nu_a(CH_2)$, I_{2880}) and CH_2-symmetric ($\nu_s(CH_2)$, I_{2844}) stretching modes at 2880 and 2844 cm^{-1}, respectively. The I_{2880}/I_{2844} ratios for 1 and 10 mM OTS films were found to be slightly higher than 1 indicating a *trans* conformation or denser packing of the alkyl chains whereas, the intensity ratio (value < 1) for 0.1 mM OTS showed a *gauche* conformation or, disorder in the C18 alkyl chains (Fig. 2A and B) (Sander et al., 2005). These results suggested a shift in the conformation of the OTS films from a disordered (liquid-like) to an ordered (crystalline-like) state on the fiber surface with an increase in the OTS concentration.

We further investigated by DCA measurements the change in surface energy of the straight fibers upon OTS functionalization. For this, the water contact angle of bare (piranha-cleaned) and OTS treated fibers were measured by immersing (advancing, θ_A) and emmersing (receding, θ_R) the fibers at a constant rate in EF water. The results showed a significant increase in the contact angle upon OTS functionalization (Table S1) indicating the increase in surface hydrophobicity due to the presence of C18 alkyl chains.

3.1.2. OTS optimization on sensor surface

Next, we studied the effect of OTS coverage on the extent of LPS loading. The above silanized surfaces were incubated with a fixed concentration of fluoro-LPS and the excess LPS was gently washed off. The microscopic analysis of these probes then revealed that the 10 mM OTS treated probes exhibited a significantly higher LPS fluorescence intensity in comparison to the bare or 1 mM OTS treated ones (Fig. 2C and D). This suggested that the crystalline modes of OTS was more suited for LPS capture than the disordered ones. In all subsequent experiments, the value of OTS concentration was thus fixed at 10 mM. It is important to note here that 10 mM is the bulk, not surface concentration. The surface wettability also improved upon LPS binding as expected (see Table S1, Supplementary material) due to the exposure of the hydrophilic polysaccharide groups on the surface. Further using SEM analysis, we found that OTS and LPS formed a uniform and smooth film on the probe surface (Fig. S3, Supplementary material). Additionally, the probes were subjected to EDAX for elemental analysis. The carbon content was found to be higher in OTS-LPS treated surface compared to only OTS functionalized probes confirming the presence of LPS (Fig. S4 and Table S2, Supplementary material).

3.1.3. Real-time monitoring of LPS binding with OTS-treated UFOPs

After establishing the best OTS conditions for maximal LPS loading, next we looked into measuring the LPS binding in real time. For this, we replaced the straight fibers with UFOPs as the fiber bending is known to significantly improve the RI sensitivity. By RI sensitivity we mean the change in light intensity passing through the fiber in response to RI changes in the bulk or microenvironment surrounding the fiber core surface (Sai and Tapanendu Kundu, 2009). The optical setup used for these experiments contained a custom-made glass flow cell in which the OTS functionalized UFOPs were dipped with varying concentrations of LPS solutions and then washed with EF water between subsequent readings (Fig. 1B). The changes in absorbance was monitored by a photodetector in real-time before and after exposure to the LPS solutions. Fig. 3A shows the time-dependent absorbance output obtained from the UFOPs at 525 nm wavelength ($A_{525\,nm}$).

Our results showed that the sensor response increased with both time and LPS concentration, reaching saturation around 15 min. It is important to note that LPS has a higher RI of ~1.50 (RI varies between 1.50 for pure and 1.33 for 90% diluted lipid A in water) compared to 1.45 RI units of bulk OTS solution (Peters et al., 2002; Seydel et al., 2000). While the bulk RI of LPS solutions (measured using a bench-top refractometer, Rudolph Research) does not vary significantly with LPS concentration considered under this study (Fig. S5, Supplementary material), the UFOP gave rise to a measurable change in the absorbance response to LPS concentration dependent binding and the corresponding RI changes in the microenvironment of the probe surface. These changes in sensor response were attributed to the high RI sensitivity of the probes to the formation of an additional LPS layer over the thin OTS film by displacing water with 1.33 RI units. The minimum detectable LPS concentration with respect to bare (OTS-free) UFOP was 0.1 μg/mL (or 10 nM, assuming10 kDa M.W. of LPS) (Fig. 3B).

3.2. Plasmonic sandwich assay for LPS detection

The evanescent wave generated at the UFOP interface can be used to further excite a chromophore such as an AuNP or a fluorophore on the fiber core surface (Sai and Tapanendu Kundu, 2009). However, compared to fluorescent labels, AuNPs labels elicit superior response owing to their high extinction coefficient. In addition, one can

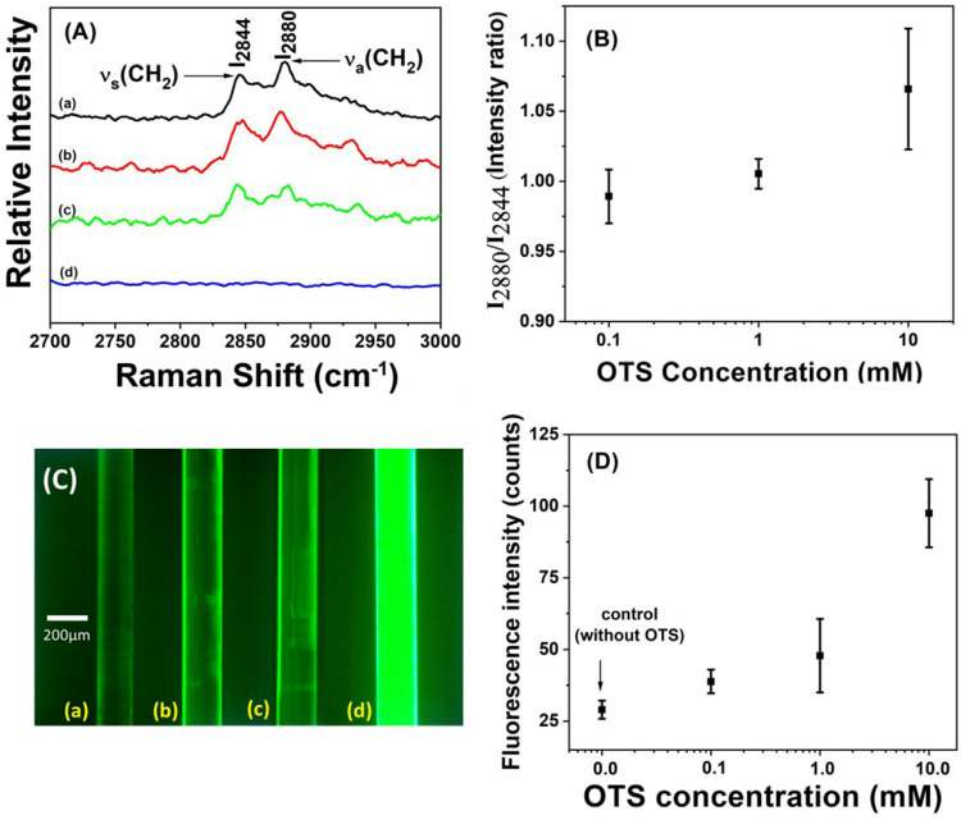

Fig. 2. Characterization of OTS-functionalized silica fiber surface for efficient LPS capture. (A) Raman spectra obtained for different OTS concentrations ((a), (b), (c) and (d) corresponds to 10, 1.0, 0.1 and 0.0 mM silane concentrations respectively). (B) Ratio of the Raman scattering intensities at 2880 and 2844 cm^{-1} as a function of OTS concentration. An increasing trend indicated desired OTS order and orientation for effective LPS capture. (C) OTS concentration-dependent fluorescence micrographs of straight silica fiber probes after treating them with 1 μg/mL of fluoro-LPS for 2 h and (D) their corresponding optical intensities. Here, (a), (b), (c) and (d) correspond to 0.0, 0.1, 1.0 and 10.0 mM OTS concentrations, respectively.

circumvent the complexities (such as return-fluorescent signal coupling through the fiber and back to detector) associated with the efficient collection of low fluorescence signal by using simpler instrumentation for optical absorption measurements. Keeping these features in mind, we next adopted a novel approach in which AuNPs coated with a well-known drug PMB were used as optical labels to quantify LPS. PMB has reportedly high affinity (K_D = 400 nM) for the phosphate groups present in the endotoxin molecule (Thomas and Surolia, 1999). Thus, the realization of this plasmonic sandwich assay was anticipated to improve both the sensitivity and specificity of our direct assay even further.

3.2.1. Drug-coated AuNP labels

The optical labels for the plasmonic sandwich assay were prepared by adding PMB to the AuNP suspensions in a 40:1 M ratio (approx.). The UV–visible absorption spectra of the conjugates showed a red-shift of ~3 nm in comparison to the bare AuNPs due to the local surface plasmon resonance (LSPR) effect suggesting the successful binding of PMB to the AuNP surface (Fig. S6, Supplementary material). Further increase in molar ratio resulted in the aggregation of AuNPs and was thus discarded.

3.2.2. Real-time monitoring of PMB-AuNP binding on LPS-treated UFOPs

Once the probes were ready, the sandwich assays were carried out by dipping the probe in an LPS solution for 25 min followed by washing in EF water twice and subsequently dipping it in PMB-AuNP suspension for 30 min. The EWA response of the UFOPs due to binding of PMB-

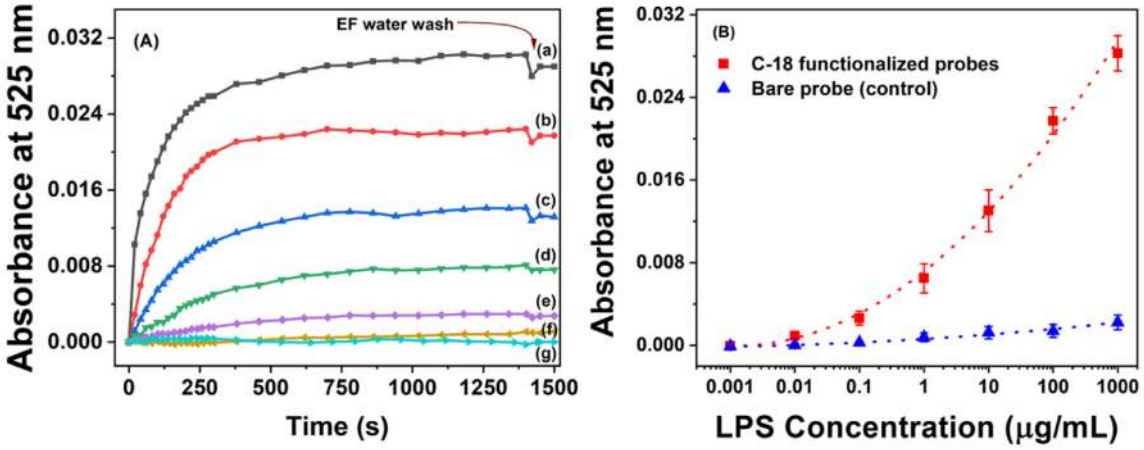

Fig. 3. Direct assay. (A) Real-time response of LPS binding to a 10 mM OTS silanized probe incubated with different LPS concentrations (μg/mL): (a) 1000, (b) 100, (c) 10, (d) 1, (e) 0.1, (f) 0.01 and (g) 0.001. The probes were gently washed after 1400 s. (B) Final absorbance response (as a result of RI changes) due to LPS binding on the OTS-functionalized and bare (without OTS) UFOP.

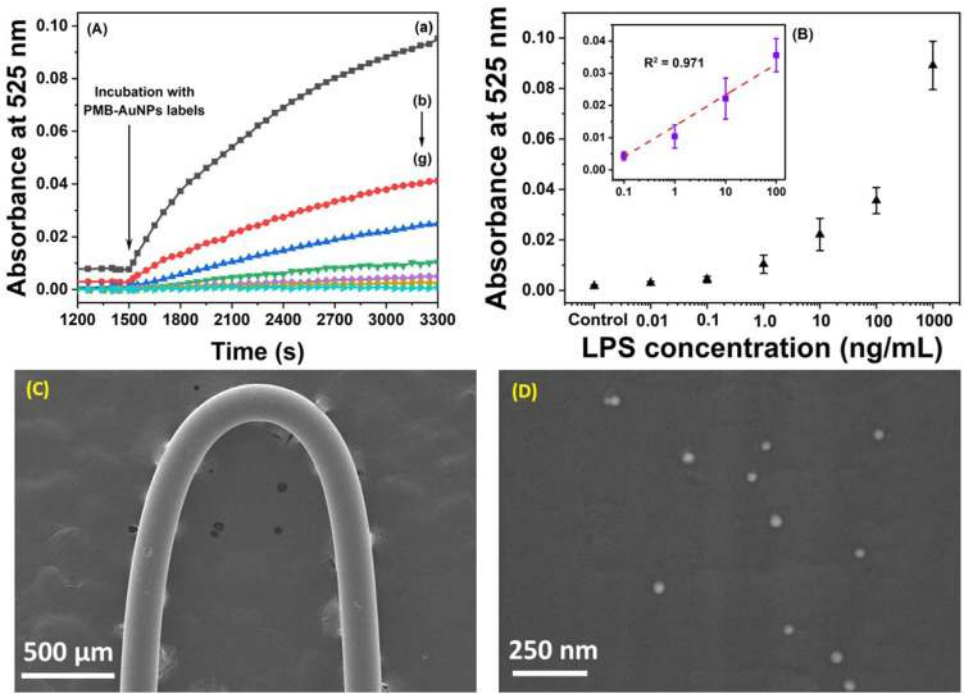

Fig. 4. Sandwich assay. (A) Time-lapsed absorbance response of PMB-AuNP binding to LPS treated probes. The LPS concentrations used were (ng/mL): (a) 1000, (b) 100, (c) 10, (d) 1, (e) 0.1, (f) 0.01 and (g) 0 (control). (B) Dose response curve on a semi-log scale. The inset shows the sensitivity of the UFOP in the linear regime. (C) and (D) SEM images of the (C) UFOP sensing region (D) PMB-AuNPs bound to the fiber probe surface.

AuNP was then recorded at 525 nm in real time. Our results showed a clear monotonic increase in absorbance over time (Fig. 4A) that varied exponentially with LPS concentration (Fig. 4B). The lowest discernable LPS concentration (over and above the bare probe) was 1 ng/mL (or, 100 pM), which was two orders of magnitude higher than the LOD obtained in the direct assay and comparable to many other LPS assays reported in the literature (Xie et al., 2016; Zhang et al., 2018). The linear sensitivity of the sensor for LPS detection between 0.1 and 100 ng/mL obtained through regression was 0.0096 $\Delta A_{525\,nm}/\Delta\log(ng/mL)$ with $R^2 = 0.97$. Further the SEM images of the U-bent probes treated with 100 ng/mL LPS confirmed the presence of AuNP on its surface (Fig. 4C and D).

3.2.3. Influence of interferents on sensor response

To further evaluate the specificity of our assay, the sensor response was monitored in the presence common biopharmaceutical interferents including amino acids such as threonine and tyrosine, lactic acid, human immunoglobulin (IgG), normal saline (NS) and dextrose normal saline (DNS). The concentrations of these contaminants were maintained 10–100 times higher than LPS. The probes were incubated in 100 ng/mL (10 nM) of LPS solution containing individual interferents followed by tagging with PMB-AuNPs labels. Our results showed that LPS in the presence of human IgG showed the minimum response however, in no case was the signal more than 15% of that obtained with LPS alone (without interferents) (Fig. 5). This was truly exciting as it showed that our assay could not only detect LPS sensitively but also highly specifically making it suitable for many biopharmaceutical applications.

3.2.4. Silver enhancement for multifold signal amplification

Our final objective was to push the sensitivity limit of our sensor response even further in order to meet the global demand for endotoxin detection. This was achieved by adopting the simple and well-known silver staining strategy in which silver is deposited on AuNPs by catalytic reduction (Gupta et al., 2007). In this, the AuNPs act as both catalysts for rapid reduction of silver ions and nucleating agents for silver deposition simultaneously. When the UFOPs were subjected to silver enhancement solution for under 3 min, their temporal and dose-dependent sensor signal showed a 36-fold rise in sensitivity at 0.344

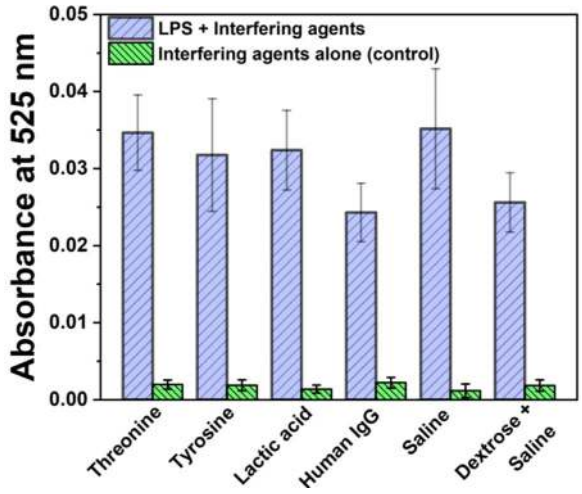

Fig. 5. Specificity of LPS sandwich assay tested by measuring the $A_{525\,nm}$ response of the sensor in the presence of common biopharmaceutical agents: threonine (1 µM), tyrosine (1 µM), lactic acid (1 µM), human IgG (10 nM), NS and DNS.

$\Delta A_{525\,nm}/\Delta\log(ng/mL)$ ($R^2 = 0.998$) with respect to the no silver reduction step and a linear response between 0.1 and 100 ng/mL LPS concentration (Fig. 6A and B). The LOD was also further lowered down to 0.4 ng/mL (or, 40 pM) which was a fair improvement than the sandwich assay format. Compared with the hitherto reports, the LOD value obtained by the C18-LPS-PMB-AuNP sandwich on fiberoptic sensors in the present study are at least one order better than the reports on LPS detection using surface plasmon resonance (SPR) techniques (Zhang et al., 2018; Abdin et al., 2015).

Separately, UV–vis absorbance characteristics of the silver enhancement process on the fiber surface was studied using a fiber optic spectrometer (Fig. S7, Supplementary material). A large red-shift in the absorbance peak was observed over time due to the rapid deposition of the silver particles on the fiber surface which was further confirmed by SEM (Fig. 6C and D).

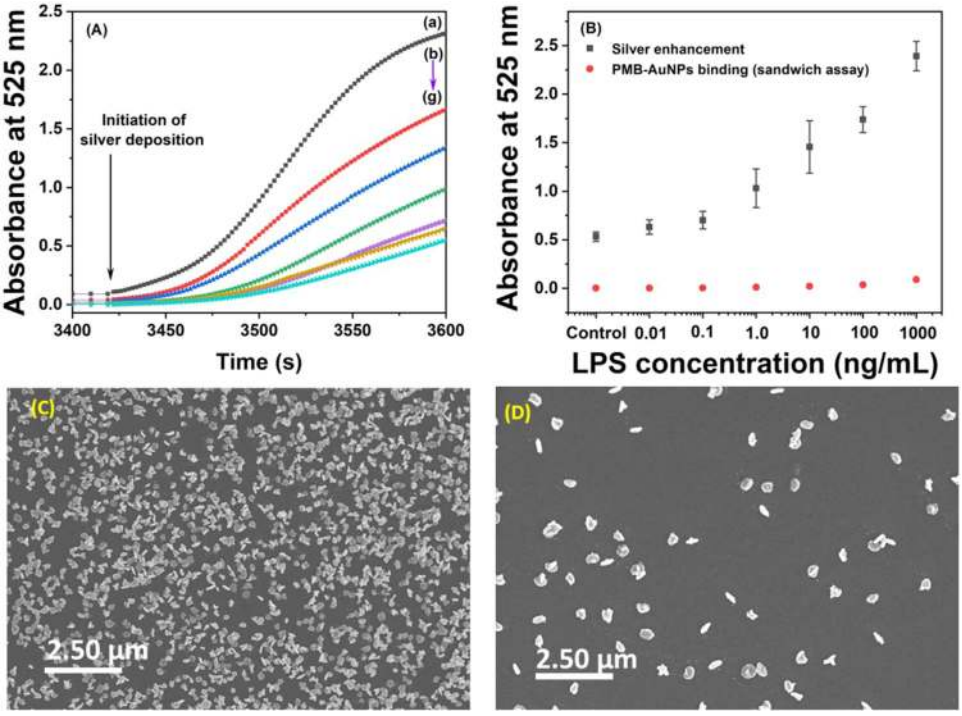

Fig. 6. Signal amplification using the silver enhancement approach. (A) Time-dependent EWA response of silver deposition on PMB-AuNP probes in the presence of different LPS concentrations (ng/mL): (a) 1000, (b) 100, (c) 10, (d) 1, (e) 0.1, (f) 0.01 and (g) 0 (control). (B) The relative dose response curves obtained with (t = 180 s) and without silver enhancement for various concentrations of LPS. (C) and (D) The corresponding SEM images of silver deposits on the fiber surface for (C) 100 ng/mL and (D) no LPS present in the assay.

4. Conclusions

We have demonstrated a simple, affordable and portable UFOP biosensor for LPS capture and detection using self-assembled C18 alkyl chains. Under the simpler direct label-free mode, the sensor was able to detect LPS concentration as low as 100 ng/mL within 15 min with a dynamic range of 0.1–1000 µg/mL of LPS, which could be highly useful for screening the pharmaceutical preparations. In the sandwich format, the sensitivity and specificity for LPS detection were improved using plasmonic drug-coated AuNPs as labels to obtain a LOD of 1 ng/mL (100 pM) within 1 h. With an additional 3 min silver enhancement-based signal amplification step, the sensitivity the sensor was improved by 36 times. The plasmonic biosensor designed in this study has at least a four-order dynamic range from 1 ng/mL (100 pM) to beyond 1000 ng/mL.

We believe that the sensor performance can be further improved by using novel ligands such as sushi peptides and aptamers in place of PMB (Posha et al., 2018; Singh et al., 2017). Also, increasing the size of the AuNPs (40 or 60 nm instead of 20 nm) is expected to improve the sensitivity (higher extinction coefficient), however at the cost of reduced assay time (lower diffusion constant) (Tu et al., 2012). Apart from LPS sensing, C18 functionalized UFOPs can be explored to study supported hybrid bilayers (SHBs) that mimic the functionality of biological cell membranes. Further, the sensors can be made more compact, miniaturized and cost-effective for onsite applications by carefully selecting the optoelectronic components such as photodiodes, LEDs and connectors. Finally, our approach can be a good alternative to the laborious and cost-prohibitive LAL assay in resource-poor settings.

Acknowledgements

H. Manoharan would like to thank Ministry of Human Resource Development (MHRD), India for financial support during his PhD program. We acknowledge HR-SEM facility in Chemical Engineering, IIT Madras funded by FIST grant from Department of Science and Technology, Government of India. We thank Mr. Allwyn (research scholar, IITM) and Mr. Dharani Balaji (project associate) for designing the LED light source and SEM analysis respectively. We acknowledge the partial support from a research grant from Indo-German Science and Technology Centre (IGSTC/2015/Multi-WAP).

Declaration of interest statement

None.

Appendix A. Supplementary material

Supplementary data associated with this article can be found in the online version at doi.org/10.1016/j.bios.2018.12.045.

References

Abdin, M.J., Altintas, E., Tothill, I.E., 2015. In silico designed nanoMIP based optical sensor for endotoxins monitoring. Biosens. Bioelectron. 67, 177–183.
Angus, D.C., Poll, T. Van Der, 2013. Severe sepsis and septic shock. N. Engl. J. Med. 369, 840–851.
Arcas, A., da, S., Dutra, F., da, S., Allil, R.C.S.B., Werneck, M.M., 2018. Surface plasmon resonance and bending loss-based U-Shaped plastic optical fiber biosensors. Sensors 18, 1–16.
Bergstrand, A., Svanberg, C., Langton, M., Nyd, M., 2006. Aggregation behavior and size of lipopolysaccharide from Escherichia coli O55: B5. Colloids Surf. B Biointerfaces 53, 9–14.
Bryant, C.E., Spring, D.R., Gangloff, M., Gay, N.J., 2010. The molecular basis of the host response to lipopolysaccharide. Nat. Rev. Microbiol. 8, 8–14.
Chandra, S., Mukherji, S., 2018. Polyaniline modified U-bent fiber optic pH sensor for physiological use. IEEE 3–4.
Chen, X., Zhou, L., Tian, K., Kumar, A., Singh, S., Prior, B.A., Wang, Z., 2013. Metabolic engineering of Escherichia coli: a sustainable industrial platform for bio-based chemical production. Biotechnol. Adv. 31, 1200–1223.
Das, A.P., Kumar, P.S., Swain, S., 2014. Recent advances in biosensor based endotoxin detection. Biosens. Bioelectron. 51, 62–75.
Dawson, E.M., 1998. The significance of endotoxin to cell culture and biotechnology. LAL Update 16, 1–4.
Divagar, M., Gowri, A., John, S., Sai, V.V.R., 2018. Graphene oxide coated U-Bent plastic optical fiber based chemical sensor for organic solvents. Sens. Actuators B. Chem. 262, 1006–1012.
FDA, U.S., 2012. Guidance for industry pyrogen and endotoxins testing: questions and answers. U. S. Food Drug Adm. 1–10.
Ferrer-miralles, N., Domingo-espín, J., Corchero, J.L., Vázquez, E., Villaverde, A., 2009. Microbial factories for recombinant pharmaceuticals. Microb. Cell Fact. 8, 8–17.
Frens, G., 1973. Controlled nucleation for the regulation of the particle size in monodisperse gold suspensions. Nat. Phys. Sci. 241, 20–23.
Gorbet, M.B., Sefton, M.V., 2005. Endotoxin: the uninvited guest. Biomaterials 26, 6811–6817.

Gowri, A., Sai, V.V.R., 2017. U-bent plastic optical fiber based plasmonic biosensor for nucleic acid detection. Proc. SPIE 10231, Opt. Sensors 10231, 1023113–1023119.
Grallert, H., Leopoldseder, S., Schuett, M., Kurze, P., Buchberger, B., 2011. EndoLISA®: a novel and reliable method for endotoxin detection. Nat. Methods 884, 3–5.
Gupta, B.D., Kant, R., 2018. Recent advances in surface plasmon resonance based fiber optic chemical and biosensors utilizing bulk and nanostructures. Opt. Laser Technol. 101, 144–161.
Gupta, S., Huda, S., Kilpatrick, P.K., Velev, O.D., 2007. Characterization and optimization of gold nanoparticle-based silver-enhanced immunoassays. Anal. Chem. 79, 3810–3820.
Huang, C.-J., Lin, H., Yang, X., 2012. Industrial production of recombinant therapeutics in Escherichia coli and its recent advancements. J. Ind. Microbiol. Biotechnol. 39, 383–399.
Jana, N.R., Gearheart, L., Murphy, C.J., 2001. Wet chemical synthesis of high aspect ratio cylindrical gold nanorods. J. Phys. Chem. B 105, 4065–4067.
Kalita, P., Bhola, A., Goel, N., Sritharan, V., Gupta, S., 2017. Heterogeneous endotoxin detection bioassay using drug–nanoparticle bioconjugates: an optimization study. Mol. Syst. Des. Eng. 2, 470–477.
Kalita, P., Dasgupta, A., Sritharan, V., Gupta, S., 2015. Nanoparticle − drug bioconjugate as dual functional affinity ligand for rapid point-of-care detection of endotoxin in water and serum. Anal. Chem. 87, 11007–11012.
Kalyanpur, M., 2002. Downstream processing in the biotechnology industry. Mol. Biotechnol. 22, 87–98.
Khatri, A., Punjabi, N., Ghosh, D., Maji, S.K., Mukherji, S., 2018. Detection and differentiation of A-Synuclein monomer and fibril by chitosan film coated nanogold array on optical sensor platform. Sens. Actuators B Chem. 255, 692–700.
Kulkarni, S.A., Mirji, S.A., Mandale, A.B., Gupta, R.P., 2005. Growth kinetics and thermodynamic stability of octadecyltrichlorosilane self-assembled monolayer on Si (100) substrate. Mater. Lett. 59, 3890–3895.
Liao, Z., Pemberton, J.E., 2008. Structure- function relationships in high-density docosylsilane bonded stationary phases by raman spectroscopy and comparison to octadecylsilane bonded stationary phases: effects of common solvents. Anal. Chem. 80, 2911–2920.
Mamat, U., Wilke, K., Bramhill, D., Schromm, A.B., Lindner, B., Kohl, T.A., Corchero, J.L., Villaverde, A., Schaffer, L., Head, S.R., Souvignier, C., Meredith, T.C., Woodard, R.W., 2015. Detoxifying Escherichia coli for endotoxin-free production of recombinant proteins. Microb. Cell Fact. 14, 1–15.
Mcgovern, M.E., Kallury, K.M.R., Thompson, M., 1994. Role of solvent on the silanization of glass with octadecyltrichlorosilane. Langmuir 1994, 3607–3614.
Peters, R.D., Nealey, P.F., Crain, J.N., Himpsel, F.J., 2002. A near edge X-ray absorption fine structure spectroscopy investigation of the structure of self-assembled films of octadecyltrichlorosilane. Langmuir 18, 1250–1256.
Petsch, D., Anspach, F.B., 2000. Endotoxin removal from protein solutions. J. Biotechnol. 76, 97–119.
Plant, A.L., 1999. Supported hybrid bilayer membranes as rugged cell membrane mimics supported hybrid bilayer membranes as rugged cell membrane mimics. Langmuir 15, 5128–5135.
Posha, B., Nambiar, S.R., Sandhyarani, N., 2018. Gold atomic cluster mediated electrochemical aptasensor for the detection of lipopolysaccharide. Biosens. Bioelectron. 101, 199–205.
Ramakrishna, B., Sai, V.V.R., 2016. Evanescent wave absorbance based U-bent fiber probe for immunobiosensor with gold nanoparticle labels. Sens. Actuators, B Chem. 226, 184–190.
Ryan, J., 2008. Endotoxins and cell culture. Corning Life Sci. Tech. Bull. 1–8.
Sander, L.C., Lippa, K.A., Wise, S.A., 2005. Order and disorder in alkyl stationary phases. Anal. Bioanal. Chem. 382, 646–668.
Schneck, E., Papp-Szabo, E., Quinn, B.E., Konovalov, O.V., Beveridge, T.J., Pink, D.A., Tanaka, M., 2009. Calcium ions induce collapse of charged O-side chains of lipopolysaccharides from Pseudomonas aeruginosa. J. R. Soc. Interface 6, S671–S678.
Seydel, U., Labischinski, H., Kastowsky, M., Brandenburg, K., 1993. Phase behavior, supramolecular structure, and molecular conformation of lipopolysaccharide. Immunobiology 187, 191–211.
Seydel, U., Oikawa, M., Fukase, K., Kusumoto, S., Brandenburg, K., 2000. Intrinsic conformation of lipid A is responsible for agonistic and antagonistic activity. Eur. J. Biochem. 267, 3032–3039.
Silin, V.I., Wieder, H., Woodward, J.T., Valincius, G., Offenhausser, a., Plant, A.L., 2002. The role of surface free energy on the formation of hybrid bilayer membranes. J. Am. Chem. Soc. 124, 14676–14683.
Singh, R., Patil, S., Singh, N., Gupta, S., 2017. Dual functionality nanobioconjugates targeting intracellular bacteria in cancer cells with enhanced antimicrobial activity. Sci. Rep. 7, 1–10.
Srivastava, S.K., Arora, V., Sapra, S., 2012. Localized surface plasmon resonance-based fiber optic U-shaped biosensor for the detection of blood glucos. Plasmonics 7, 261–268.
Thomas, C.J., Surolia, A., 1999. Kinetics of the interaction of endotoxin with polymyxin B and its analogs: a surface plasmon resonance analysis. FEBS Lett. 445, 420–424.
Tu, M.H., Sun, T., Grattan, K.T.V., 2012. Optimization of gold-nanoparticle-based optical fibre surface plasmon resonance (SPR)-based sensors. Sens. Actuators B Chem. 164, 43–53.
Sai, V.V.R., Tapanendu Kundu, S.M., 2009. Novel U-bent fiber optic probe for localized surface plasmon resonance based biosensor. Biosens. Bioelectron. 24, 2804–2809.
Velkov, T., Thompson, P.E., Nation, R.L., Li, J., 2010. Structure − activity relationships of polymyxin antibiotics. J. Med. Chem. 53, 1898–1916.
Whitfield, C., Trent, M.S., 2014. Biosynthesis and export of bacterial lipopolysaccharides. Annu. Rev. Biochem. 83, 99–125.
Williams, K.L., Roberts, K., Nnalue, N., Pearson, F.C., 2007. Endotoxins: Pyrogens, LAL Testing, and Depyrogenation, third ed. CRC Press, Boca Raton, Florida, pp. 321.
Xie, P., Zhu, L., Shao, X., Huang, K., Tian, J., Xu, W., 2016. Highly sensitive detection of lipopolysaccharides using an aptasensor based on hybridization chain reaction. Sci. Rep. 6, 1–8.
Zhang, J., Khan, I., Zhang, Q., Liu, X., Dostalek, J., Liedberg, B., Wang, Y., 2018. Lipopolysaccharides detection on a grating-coupled surface plasmon resonance smartphone biosensor. Biosens. Bioelectron. 99, 312–317.